

# Residual stress effects on plastic deformation and interfacial fracture in thin-film structures

Christopher S. Litteken, Sven Strohband, Reinhold H. Dauskardt \*

*Department of Materials Science and Engineering, Stanford University, 416 Escondido Mall, Bldg. 550, Stanford, CA 94305-2205, USA*

Received 18 August 2004; received in revised form 7 January 2005; accepted 7 January 2005

## Abstract

Residual stress in ductile thin films is shown to significantly affect the extent of film plasticity and interfacial fracture energy during debonding in thin-film structures. Specifically, the interfacial fracture resistance of a TaN/SiO<sub>2</sub> interface in a thin-film structure containing an adjacent ductile Cu film with varying residual stress is compared to predictions from computational models. The fracture energy of the TaN/SiO<sub>2</sub> interface increased by 50% for structures containing a Cu film in compression compared to similar structures with the film in tension. The effect of residual stress on interfacial adhesion is rationalized in terms of the onset of yielding within the Cu film, which affects the contribution from plastic energy dissipation to the total interface fracture energy.

© 2005 Acta Materialia Inc. Published by Elsevier Ltd. All rights reserved.

*Keywords:* Thin films; Toughness; Internal stresses; Fracture; Plastic deformation

## 1. Introduction

Interfacial fracture resistance of thin-film structures is often dominated by plastic energy dissipation in adjacent ductile layers. Recent simulations suggest that compressive residual stress in the ductile layer may significantly increase plasticity and fracture resistance while tensile stresses reduce plasticity and fracture resistance [1]. These simulations considered the case of an interfacial debond separating a thin elastic layer from an adjacent plastically deforming film. The results were surprising because intuitively it may be expected that when tensile crack tip stress fields are superimposed on tensile residual stresses in the ductile film, more rather than less plasticity would result. The predicted behavior was rationalized in terms of the deviatoric stress in the ductile film which was found to decrease in the case of tensile residual stresses, and increase in the case of com-

pressive residual stresses. To date, experimental validation of this unexpected effect has not been reported.

The phenomenon may be particularly important for emerging thin-film device structures, such as those found in microelectronic interconnect structures, where interfacial fracture resistance is crucial for interconnect reliability and residual stresses in metal layers may be large. In the case of Cu dual damascene structures, thin Cu films are encapsulated by elastic barrier layers, such as TaN, and insulated by a low-*k* dielectric material, typically a brittle glass. It has been established that the interface fracture energy,  $G_c$ , of a normally brittle low-*k* dielectric/barrier layer interface may be significantly increased through plastic energy dissipation in nearby thin ductile films, such as Cu or organic low-*k* materials [2–4]. The plastically deforming film may be adjacent to the debonding interface or separated by a thin elastic layer. The contribution to  $G_c$  from plastic energy dissipation,  $G_{pl}$ , has been shown to be strongly dependent on parameters such as the ductile film thickness,  $h_d$ , the intrinsic interfacial adhesion,  $G_0$ , the ductile layer yield stress,  $\sigma_{ys}$ , the elastic layer thickness, and the

\* Corresponding author. Tel.: +1 650 725 0679; fax: +1 650 725 4034.

*E-mail address:* [dauskardt@stanford.edu](mailto:dauskardt@stanford.edu) (R.H. Dauskardt).

aspect ratio of lithographically patterned lines [3–7]. It has also been observed that the  $G_{pl}$  contribution decreases with decreasing ductile film thickness due to a combination of thin-film strengthening mechanisms and the elastic constraint provided from adjacent layers [3,4,8,9].

The intent of the present study was to investigate the effect of varying residual stress on the contribution from plastic energy dissipation to interfacial fracture energy. A thin-film stack containing a Cu film of varying thickness and a Ta/TaN/SiO<sub>2</sub> barrier was prepared on Si wafers. The structures were thermally cycled to induce large variations in the Cu film's biaxial residual stress from –59 to 306 MPa. X-ray diffraction techniques were used to characterize the residual stress in the Cu layer. The four-point bend adhesion technique was employed to determine the TaN/SiO<sub>2</sub> interface fracture energy,  $G_c$  [2]. Results describing the interfacial fracture energy of the TaN/SiO<sub>2</sub> interface are presented as a function of Cu film thickness and residual stress.

The values of  $G_c$  for the TaN/SiO<sub>2</sub> interface were dominated by energy dissipated through plastic deformation of the adjacent Cu film and were sensitive to the Cu film residual stress.  $G_c$  increased by ~50% when the Cu film was residually stressed in compression compared to an identical film in tension. Simulations using material properties and film thicknesses similar to the thin-film stack employed in the experimental study are also presented. The experimental results closely match those predicted by simulation for a range of Cu film thicknesses and residual stresses. The trends in adhesion from both the experimental and theoretical studies are explained in terms of onset of yielding within the Cu film and the resulting increase in plastic energy dissipation.

## 2. Experimental procedures

A schematic illustration of the thin-film structure employed is shown in Fig. 1. A 300 nm layer of thermal SiO<sub>2</sub> was grown on 200 mm diameter Si wafers. An elastic bilayer barrier comprised of 15 nm of TaN followed

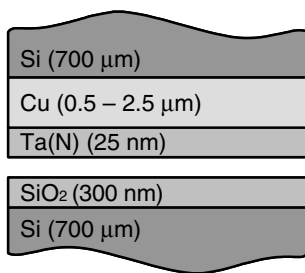


Fig. 1. Schematic of the sandwiched thin-film structure containing a Cu film of varying thickness with a debonded TaN/SiO<sub>2</sub> interface.

by 10 nm of Ta was deposited by physical vapor deposition (PVD) on the SiO<sub>2</sub>. Cu films with total thickness of either 0.25 or 1.15 μm were then deposited on the Ta surface using a Cu PVD seed and electroplating process. To produce specimens for four-point bend adhesion measurements, 40 mm square samples were cleaved from the wafers. The squares were then bonded together at 500 °C for 4 h at a pressure of 14 MPa in a reducing gas of 96% N and 4% H. The resulting sandwich structures contained Cu films with a total thickness of 0.5, 1.4 and 2.3 μm.

Individual four-point bend specimens were machined from the sandwiched wafers using a high speed dicing saw with dimensions of 4 mm wide and 40 mm long with a central notch machined to within ~100 μm of the TaN/SiO<sub>2</sub> interface. The specimens were annealed in a N<sub>2</sub> environment for 4 h at 500 °C and cooled to room temperature. Following annealing, selected specimens were quenched in liquid N<sub>2</sub> at –196 °C for 30 min and then allowed to warm to room temperature. It has been observed that thermally cycling Cu in this fashion creates tensile stresses in the Cu films following the high temperature anneal and compressive stresses following the low temperature quench [10].

Thin-film adhesion testing was conducted under mixed-mode loading conditions using the four-point bend technique [2,11]. Specimens were loaded under displacement control in an articulating four-point bend fixture. The four-point bend adhesion measurements were conducted with a crosshead displacement rate of 0.5 μm/s. Interfacial debonds from four different beams were propagated along the TaN/SiO<sub>2</sub> interface for each experimental condition. Multiple measurements of adhesion were made on each beam by changing the position of the loading pins. Following adhesion measurements, the resulting fracture surfaces were characterized by X-ray photoelectron spectroscopy (XPS), to verify the location of the debond path at the TaN/SiO<sub>2</sub> interface.

X-ray diffraction (XRD) techniques were used to quantify the strain in the Cu films by measuring the interplanar spacings of select crystallographic planes. Measurements were made on two unbonded substrates cleaved from the wafer containing a 1.15 μm Cu film following the identical thermal cycling procedures previously described. A Phillips MRD was used to measure the diffracted X-ray intensity as a function of the angle between the incident X-ray beam and film surface,  $\theta$ , and the angle between the film surface normal and normal of the diffracting planes,  $\psi$  [12,13]. The interplanar spacing,  $d$ , for the family of Cu {311} planes was measured at  $\psi = 29.50^\circ$ ,  $58.51^\circ$ , and  $79.98^\circ$  for both substrates. Using the well-established  $\sin^2[\psi]$  technique for fiber textured  $\langle 111 \rangle$  metal films, the unstrained lattice parameter,  $d_0$ , and the residual stress,  $\sigma_r$ , in the Cu films were calculated.

### 3. Simulation procedure

The simulation procedure was similar to the technique used previously for a more comprehensive exploration of the effect of residual stress on the macroscopic interface fracture energy for thin-film structures [1]. Since a simulation of the full fracture sample geometry would involve an impractical number of elements, a multiscale approach as shown in Fig. 2 was employed. The Cu layer and the adjacent Ta(N) barrier layer were embedded within a circular region of radius  $r_0 = 50 \mu\text{m}$  around the tip of the debond. The layers were meshed using 4-noded quadrilateral elements and the circular region was meshed using Delaunay triangulization. The overall mesh consisted of  $\approx 50,000$  elements with the smallest element size  $h_{\min} \approx 8 \text{ nm}$  and the ratio between the smallest and largest element sizes  $h_{\min}/h_{\max} \approx 200$ .

For the purposes of the simulation the Ta and TaN layers were combined as one elastic layer of thickness  $h_B = 25 \text{ nm}$  with average material properties. The thickness of the Cu layer was varied between 0.2 and 2.5  $\mu\text{m}$ . Displacement boundary conditions determined from the asymptotic stress field solution for a crack in an isotropic linearly elastic medium were applied on the perimeter of the circular zone in terms of the applied Mode I and II stress intensity factors,  $K_I$  and  $K_{II}$ , respectively. For the simulations a mode mixity of  $\Psi = 43^\circ$  was employed that is the same as that imposed using the four point bend specimen configuration described in the experimental section. The circular zone was chosen to be large compared to the film thickness and the asymptotic displacement field is therefore not significantly altered by the embedded thin-layered structure.

For the elastic barrier layer and the surrounding Si matrix a finite strain Kirchoff–St. Venant model was used and the Cu layer was modeled by a finite strain,  $J_2$  plasticity model with linear isotropic hardening. The yield criterion for the copper layer was

$$f(\boldsymbol{\tau}, \alpha) := \|\text{dev}(\boldsymbol{\tau})\| - \sqrt{\frac{2}{3}}\kappa(\alpha) \leq 0, \quad (1.1)$$

where  $\boldsymbol{\tau}$  is the Kirchoff stress tensor,  $\alpha$  is the equivalent plastic strain and the isotropic hardening function  $\kappa(\alpha)$  is given by

$$\kappa(\alpha) = \sigma_{ys} + H\alpha, \quad (1.2)$$

where  $H$  is the isotropic hardening modulus. A more complete description of this plasticity model can be found in [14,15].

The debond was modeled using cohesive zone elements (CZE) with a stress separation function of

$$\sigma(\delta) = A\delta e^{-\frac{\delta}{B}}, \quad (1.3)$$

where  $A$  and  $B$  are constants and  $\delta$  is the displacement of formerly closed points of the cohesive elements. The employed cohesive law is isotropic in the sense that normal and shear displacements within the CZE elements have an equal effect on the resulting tractions on the interface. The constants  $A$  and  $B$  are related to the intrinsic fracture energy  $G_0$  and the peak cohesive stress  $\sigma_C$  at the interface by

$$G_0 = AB^2 \quad \text{and} \quad \sigma_C = \frac{AB}{e}. \quad (1.4)$$

The simulation progresses by increasing the applied far field load and subsequently reestablishing equilibrium in the modeling zone of radius  $r_0$ . Crack tip extension was detected by monitoring the location of the peak tractions at the interface. In the event of crack tip movement, the asymptotic displacement boundary conditions were updated to account for the new crack tip position. The procedure was continued until a plateau value of the debond resistance curve was reached. The plateau value was taken as the interface fracture energy,  $G_C$ .

In the range of Cu films currently investigated, the yield stress of the Cu films has been measured with wafer curvature techniques to be inversely proportional to the layer thickness and can be described as

$$\sigma_{ys} = \beta + \frac{\alpha}{h_d}, \quad (1.5)$$

where  $\alpha$  and  $\beta$  are materials constants used to fit the experimental data [9,16]. The yield stress of the simulated Cu films taken from published values is plotted as a function of Cu layer thickness in Fig. 3. The yield data for Model 1 in Fig. 3 is taken directly from the literature [16]. For Model 2 a similar slope of the yield

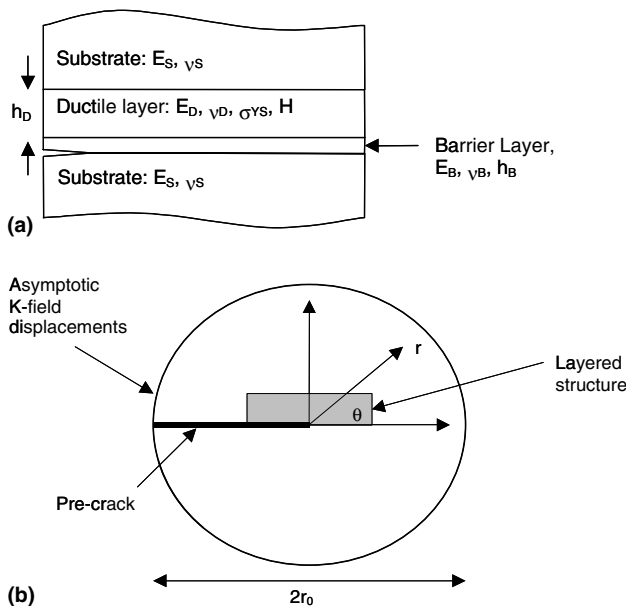


Fig. 2. Schematic illustration of the thin-film structure investigated showing: (a) the debonding interface separated from the ductile layer by a thin barrier layer; (b) the circular zone containing the FEM mesh.

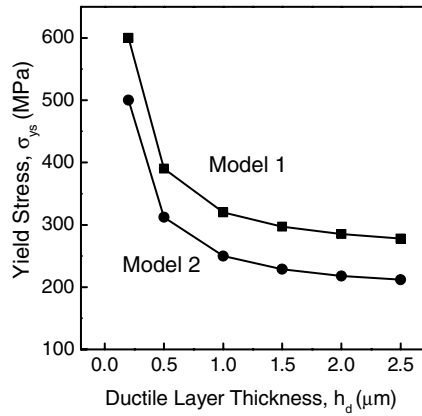


Fig. 3. Cu layer yield stress as function of the layer thickness.

Table 1  
Material and cohesive zone properties employed in the simulations

|         | $G_0$ (J/m <sup>2</sup> ) | $\sigma_c$ (GPa) | $H$ (GPa) | $\alpha$ (MPa/μm) | $\beta$ (MPa) |
|---------|---------------------------|------------------|-----------|-------------------|---------------|
| Model 1 | 10                        | 1.6              | 5         | 70                | 250           |
| Model 2 | 5                         | 1.6              | 1         | 60                | 1887          |

Table 2  
Material properties used in the simulation

| Material            | Modulus (GPa) | Poisson's ratio | Yield stress                         |
|---------------------|---------------|-----------------|--------------------------------------|
| Si/SiO <sub>2</sub> | 100           | 0.25            | None                                 |
| Ta(N)               | 550           | 0.33            | None                                 |
| Cu                  | 128           | 0.34            | Variable (see Eq. (1.5) and Table 1) |

The Ta/TaN layers are modeled as one single elastic layer with average mechanical properties. All layers, except for the Cu layer, are modeled as purely elastic layers.

stress versus the inverse of the layer thickness was assumed but the values were shifted to lower yield stresses as obtained by microtensile experiments [17]. Cohesive zone properties of the interface were set to previously published values for the two models [9]. A summary of the parameters used in Models 1 and 2 is presented in Table 1. The same elastic properties were used for both models and values are summarized in Table 2. The residual stress was introduced in the Cu layer by specifying an inelastic strain in the layer that results in an in-plane, biaxial residual stress. Details of this procedure have been previously published [1].

## 4. Results and discussion

### 4.1. XRD stress measurement

The Cu films were found to have a  $\langle 111 \rangle$  texture based on symmetric  $2\theta$  scans ( $\psi = 0^\circ$ ) collected on each

substrate before and after thermal cycling. Significant intensities of diffracted X-rays were observed exclusively for angles satisfying the Bragg condition corresponding to Cu  $\langle 111 \rangle$  planes. Similar observations of strong  $\langle 111 \rangle$  fiber texture, using off-axis rocking curve XRD techniques, were made during other investigations of electro-deposited Cu films on Ta(N) barriers following a high temperature anneal [16]. It was assumed that the Cu films were sufficiently thick (1.15 μm) to avoid reflections from the substrate and barrier layer for all presently discussed XRD scans.

A rigorous derivation of the  $\sin^2[\psi]$  technique to determine residual stress of textured metal films has been extensively reported elsewhere [10,12,13,16,18]. As expected from the analysis, the  $d$  spacings for a given thermal cycle lie on a straight line with a slope  $m$ , when plotted against  $\sin^2[\psi]$  as shown in Fig. 4. The equal biaxial stress,  $\sigma_r$ , in the  $\langle 111 \rangle$  Cu film is given by

$$\sigma_r = \frac{m}{d_0} C_{44}, \quad (1.6)$$

where the shear stiffness of Cu,  $C_{44} = 75$  GPa [16]. An accurate measurement for  $d_0$  can be made from the intersection of the linear fits in Fig. 4 [19]. The unstressed lattice parameter,  $d_0$ , for the  $\{311\}$  Cu planes was determined to be 1.0899 Å. In the case of  $\langle 111 \rangle$  textured films, the residual stress in the film can be assumed to be an equal biaxial stress since the stiffness of  $\langle 111 \rangle$  plane is isotropic. The residual stress in the Cu film was determined to be 306 MPa for the annealed films and  $-59$  MPa for the quenched films, in close agreement with studies of Cu films after similar thermal cycling [10].

### 4.2. The effect of residual stress on $G_c$

The experimentally measured  $G_c$  values of the TaN/SiO<sub>2</sub> interface for structures containing the tensile and

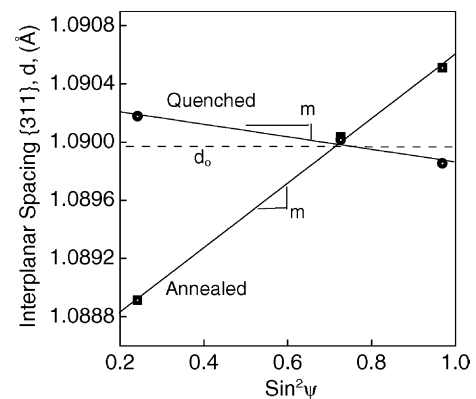


Fig. 4. Interplanar spacing,  $d$ , for the Cu  $\{311\}$  planes as a function of  $\sin^2[\psi]$ . The values of  $d$  lie on a straight line for each thermal cycling condition.

compressive Cu layers are shown in Fig. 5(a) as a function of the Cu film thickness. The simulation results are included in the figure for comparison. In all cases, XPS characterization of the debonded surfaces revealed that the TaN/SiO<sub>2</sub> interface was fractured. The value of  $G_c$  was  $\sim 10$  J/m<sup>2</sup> for the 0.5  $\mu$ m thick Cu films in tension and slightly higher at  $\sim 11$  J/m<sup>2</sup> for the Cu film in compression. With increasing Cu thickness, however,  $G_c$  values were observed to increase significantly. Most notably, the  $G_c$  values of structures containing the Cu films with compressive residual stress were markedly higher than those containing the same thickness Cu films in tension. For structures with the thickest Cu films,  $G_c$  was observed to be  $\sim 19$  J/m<sup>2</sup> for the Cu film in tension, and  $G_c \sim 29$  J/m<sup>2</sup> for the Cu film in compression. The value of  $G_c$  therefore increased by  $\sim 50\%$  when

the Cu film residual stress was decreased from 306 to  $-59$  MPa.

We note initially that the residual stress in the thin-film structures does not affect the measured values of  $G_c$  due to a change in strain energy stored in the specimens. In the sandwiched four-point bend specimen configuration, residual stresses in the thin-films are prevented from significantly contributing to the measured fracture energy by the elastic Si substrates as previously demonstrated [2]. We also note that the residual stresses do not directly oppose opening of the crack plane which might result in increased apparent fracture resistance. Previous studies have found the fracture toughness of bulk Al alloys can be significantly altered as a result of thermal cycling intended to impose varying residual stress states [20]. However, the distribution of compressive residual stresses in the bulk Al specimens that elevate the measured fracture energy do not exist in the present thin-film layers. Indeed, the residual stresses act in the plane of the film and do not oppose the applied stress as they may in the case of bulk specimens.

The variation of  $G_c$  values observed for the TaN/SiO<sub>2</sub> interface with Cu layer thickness and residual stress levels is associated with different amounts of plastic deformation in the Cu layers. These result in different  $G_{pl}$  contributions to  $G_c$ . The  $G_{pl}$  contribution is related to the size of the plastic zone in the ductile layer. In the absence of residual stress, our previous simulations on similar thin-film structures suggested that the extent of the plastic zone and  $G_{pl}$  contribution will be limited by the thickness of the ductile layer,  $h_d$ , when  $h_d < 2r_0$  [1], where  $r_0$  is a modeling length scale related to the size of the plastic zone that would form in the bulk ductile material [21]. Such ductile film thickness effects on  $G_c$  have been observed for thin-film structures containing metal and polymer ductile layers [3,4,9]. In the presence of tensile residual stresses in the ductile layer, the reduced plasticity leads to an earlier insensitivity to the ductile film thickness, and in the case of compressive film stresses, the thickness dependence persists to much larger values depending on the level of the residual stress [1]. These observations are consistent with the effects of Cu layer thickness and residual stress measured experimentally in the present study. We note for the present Cu films that  $\sigma_{ys}$  is strongly thickness dependent and hence influences the value of  $r_0$  for each of the film thicknesses examined. The film thickness effects on the yield properties of Cu films has been extensively investigated [3,16,22–24]. The present results for  $G_c$  are therefore entirely consistent with plasticity effects in the Cu layer.

Extrapolation of the observed data to a Cu film of zero thickness suggests that  $G_0$  for the TaN/SiO<sub>2</sub> interface is between 5 and 10 J/m<sup>2</sup>. In the absence of crack tip plasticity in adjacent ductile layers, fracture energies of barrier/SiO<sub>2</sub> interfaces are generally reported in this

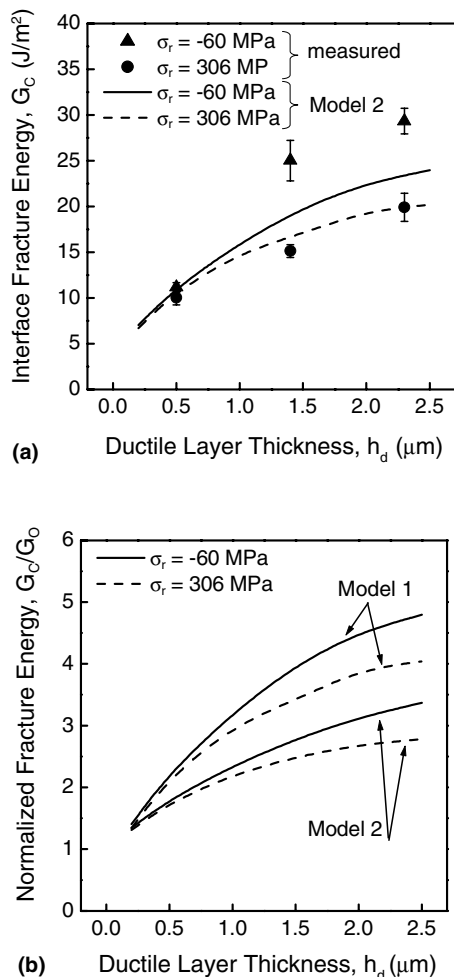


Fig. 5. TaN/SiO<sub>2</sub> interfacial fracture energy as a function of adjacent Cu layer thickness showing: (a) a comparison of measured  $G_c$  values with predicted behavior using Model 2, and (b) simulation results indicating the effect of residual stress in the Cu layer on the normalized fracture energy ( $G_c/G_0$ ) using the material and interfacial properties from Tables 1 and 2. Models 1 and 2 provide reasonable upper and lower bounds for the relevant Cu yield properties and TaN/SiO<sub>2</sub> interface cohesive zone parameters.

range and depend on glass density, composition, interface chemistry and structure. For example, we previously reported  $G_0$  values of  $\sim 5\text{--}10\text{ J/m}^2$  for similar Ta(N)/SiO<sub>2</sub> interfaces [3,9] depending on interface chemistry. In addition, we note that the bulk fracture toughness of dense SiO<sub>2</sub> is at the upper limit of the same range [25,26]. Previously published studies also determined the values of  $G_c$  for the 0.5  $\mu\text{m}$  thick Cu films are likely to exhibit some contribution from plasticity, perhaps as much as  $5\text{ J/m}^2$  [3]. In addition, the value is clearly at least  $1\text{ J/m}^2$  larger for the Cu film in compression compared to the same film in tension. These observations suggest that the value of  $G_0$  for the TaN/SiO<sub>2</sub> interface is likely to be lower in the  $5\text{--}10\text{ J/m}^2$  range obtained from the extrapolation and closer to the parameters chosen for Model 2 described below.

The effect of residual stress in the Cu layer on the measured  $G_c$  values are clearly consistent with predictions from previously reported simulations [1]. The results from the present simulations of the structure using material and cohesive zone properties listed in Table 1 are consistent with the values and trends observed experimentally for  $G_c$  (Fig. 5). Model 2, which assumes a lower value of  $G_0$  and a weaker Cu layer with lower hardening modulus, appears to capture the increasing  $G_c$  value with tensile Cu layer thickness most accurately, but under-predicts the increase in  $G_c$  observed for the compressively stressed Cu layer. Model 1 predicts similar trends but is generally less consistent with the values of the measured data, and again under-predicts the difference between the tensile and compressive Cu layers. There is clearly sufficient uncertainty in the values of the material and cohesive zone properties listed in Tables 1 and 2 that a closer fit should not be anticipated without artificially adjusting the parameters. Currently all the effects of Cu layer thickness and thermal treatments on the constitutive behavior of the Cu layer are unknown.

More importantly, however, the present study serves to experimentally verify the prediction that residual stress in ductile layers may significantly affect the extent of local crack tip plasticity during debonding of an adjacent interface, even if it is separated from the ductile layer by a thin elastic layer. The somewhat surprising results are that compressive film stresses lead to more plasticity in the ductile layer and higher  $G_c$  values, while tensile stresses lower the plasticity contribution to  $G_c$ . These results are unexpected because it might be intuitively expected that the superposition of tensile crack tip stress fields and tensile film stresses would lead to more, rather than less, plasticity in the ductile layer. The effect is associated with the deviatoric component of the stress state ahead of the crack tip, which decreases in the case of the tensile film stresses, thus inhibiting yielding of the layer.

## 5. Conclusion

The effect of varying residual stress in a ductile Cu layer on the interfacial fracture energy of an adjacent TaN/SiO<sub>2</sub> interface in a thin film structure was investigated. The interface fracture energy,  $G_c$ , was shown to increase with increasing Cu layer thickness, indicative of plastic deformation in the Cu layer. More importantly, however, experimental and simulation results indicated that varying the residual stress of the ductile film significantly affects the extent of plastic energy dissipation and consequently  $G_c$ . For structures with 2.3  $\mu\text{m}$  thick Cu films,  $G_c$  was determined to be  $\sim 19\text{ J/m}^2$  for the Cu films with a 306 MPa tensile biaxial film stress, and  $\sim 29\text{ J/m}^2$  for the Cu film with a compressive film stress of  $-59\text{ MPa}$ . The value of  $G_c$  therefore increased by  $\sim 50\%$  when the Cu film residual stress was decreased from 306 to  $-59\text{ MPa}$ . The trends are explained in terms of the onset of yielding within the ductile Cu film. The deviatoric stress component in the ductile film resulting from the superposition of the crack tip stress fields and the film stress increases in the case of compressive stresses and decreases in the case of tensile stresses. The resulting effects on plasticity in the ductile film are shown to have a significant effect on the resulting value of  $G_c$ .

## Acknowledgements

This work was supported by the Director, Office of Energy Research, Office of Basic Energy Sciences, Materials Science Division of the US Department of Energy under Contract No. DE-FG03-95ER45543A009. The authors gratefully acknowledge useful discussions and specimens provided by Drs. A. Bodke, N. Krishna, and LiQun Xia, Applied Materials Corporation, Santa Clara, CA.

## References

- [1] Strohsband S, Dauskardt R. *Interf Sci* 2003;11:309–17.
- [2] Dauskardt RH, Lane M, Ma Q, Krishna N. *Eng Fract Mech* 1998;61:141–62.
- [3] Lane M, Dauskardt RH, Vainchtein A, Gao H. *J Mater Res* 2000;15:2758–69.
- [4] Litteken CS, Dauskardt RH. *Int J Fract* 2003;119:475–85.
- [5] Wei Y, Hutchinson JW. *J Mech Phys Sol* 1997;45:1137–59.
- [6] Tymiak NI, Volinsky AA, Kriese MD, Downs SA, Gerberich WW. *Metall Mater Trans A* 2000;31A:863–72.
- [7] Evans AG, Hutchinson JW, Wei Y. *Acta Mater* 1999;47:4093–113.
- [8] Volinsky AA, Tymiak NI, Kriese MD, Gerberich WW, Hutchinson JW. *Fracture and ductile vs. brittle behavior – theory, modeling and experiment*. Boston (MA); 1999. p. 277–90.
- [9] Lane M, Dauskardt RH, Krishna N, Hashim I. *J Mater Res* 2000;15:203–11.

- [10] Florando JN, Nix WD. Dislocations and deformation mechanisms in thin films and small structures. San Francisco (CA); 2001. p. 1–6.
- [11] Ma Q, Bumgarner J, Fujimoto H, Lane M, Dauskardt RH. Materials reliability in microelectronics VII. San Francisco (CA); 1997. p. 3–14.
- [12] Noyan IC, Huang TC, York BR. *Crit Rev Sol State Mater Sci* 1995;20:125–77.
- [13] Clemens BM, Bain JA. *MRS Bull* 1992;17:46–51.
- [14] Simo JC. *Comput Meth Appl Mech Eng* 1988;66:199–219.
- [15] Simo JC. *Comput Meth Appl Mech Eng* 1988;68:1–31.
- [16] Vinci RP, Zielinski EM, Bravman JC. *Thin Solid Films* 1995;262:142–53.
- [17] Hommel M, Kraft O, Baker SP, Arzt E. Materials science of microelectromechanical systems [MEMS] devices. Boston (MA); 1998. p. 133–8.
- [18] Flinn PA, Chien C. *J Appl Phys* 1990;67:2927–31.
- [19] Cornella G, Lee S-H, Nix WD, Bravman JC. *Appl Phys Lett* 1997;71:2949–51.
- [20] Ibrahim RN, Sayers RD, Ischenko D. *Eng Fract Mech* 1998;59:215–24.
- [21] Hutchinson JW, Evans AG. *Acta Mater* 2000;48:125–35.
- [22] Doerner MF, Gardner DS, Nix WD. *J Mater Res* 1986;1:845–51.
- [23] Nix WD. *Metall Trans A* 1989;20:2217–45.
- [24] Kretschmann A, Kuschke WM, Baker SP, Arzt E. Thin films: stresses and mechanical properties VI. Pittsburgh (PA); 1997. p. 59–64.
- [25] Lucas JP, Moody NR, Robinson SL, Hanrock J, Hwang RQ. *Scripta Metall Mater* 1995;32:743–8.
- [26] Ritter JE, Fox JR, Hutko DI, Lardner TJ. *J Mater Sci* 1998;33:4581–8.